Astron. Astrophys. 328, 175–186 (1997)

ASTRONOMY
AND
ASTROPHYSICS

High resolution infrared spectroscopy of CN and NH lines: nitrogen abundance in oxygen-rich giants through K to late M⋆

W. Aoki[1,2] **and T. Tsuji**[1]

[1] Institute of Astronomy, The University of Tokyo, Osawa, Mitaka, Tokyo 181, Japan
[2] Department of Astronomy, School of Science, The University of Tokyo, Bunkyo-ku, Tokyo 113, Japan

Received 2 January 1997 / Accepted 7 April 1997

Abstract. The analyses of high resolution infrared spectra have been done for CN lines in oxygen-rich cool evolved stars including 2 K giants, 20 M giants and 1 S-type star. Since CN lines analyzed in the present work are weak and resolved well, they are appropriate for quantitative analyses. CN lines of $\Delta v = -2$ and -1 sequences (red system) which are in the K- and the H-window regions, respectively, give the consistent nitrogen abundance for each star. The analyses of NH lines in the L-window region have been done for 5 late M giants for which CN lines have been also analyzed. Although the triplet structure of NH lines cannot be fully resolved, they are preferable because determination of nitrogen abundance is almost independent of other elemental abundances while nitrogen abundance based on CN depends on carbon abundance. The nitrogen abundances derived from NH for late M giants agree well with those from CN for which we adopt 7.75 eV as the dissociation energy in the analysis.

The results show that the nitrogen abundances in late M giants are larger than those in early M giants while decrease of the carbon abundance was found in late M giants by our previous work (Tsuji 1991). These variations of abundances can not be explained by the first dredge-up model but require additional processing by the CN cycle and mixing after the first dredge-up. However, there is no obvious evidence of other processes such as the 3α-process and subsequent hot bottom burning in our program stars. Such variation of the carbon and nitrogen abundances is not well understood by the present evolutionary models of low-mass and intermediate-mass stars.

Key words: stars: abundances – stars: atmospheres – stars: late-type – stars: AGB and post AGB

⋆ Table 10 is only available in electronic form at the CDS (Strasbourg) via anonymous ftp to cdsarc.u-strasbg.fr (130.79.128.5) or via http://cdsweb.u-strasbg.fr/Abstract.html

1. Introduction

Studies of the chemical composition of cool stars on red giant branch (RGB) and on asymptotic giant branch (AGB) which are in evolved states of low-mass and intermediate-mass stars have basic importance to clarify stellar evolution as well as chemical evolution of the Galaxy. As is well known the abundances of carbon, nitrogen, oxygen and their isotopes in cool giants suffer large changes through their evolutions and these stars probably have been contributing to the enrichments of these elements in the Galaxy. Especially the origins of carbon and nitrogen in the Galactic chemical evolution have not yet been clarified well compared with that of oxygen which is explained well by the nucleosynthesis in the type II supernova events.

On the other hand the evolution and nucleosynthesis of low-mass and intermediate-mass stars have not been well understood yet. The carbon, nitrogen and oxygen abundances of RGB stars can be explained by the theory of the first dredge-up (Lambert & Ries 1981). However the interpretation of the carbon isotope ratio in red giants has been controversial for a long time and recently an explanation was proposed by Charbonnel (1995) (see Sect. 6.2). Further the evolution along AGB, through which low-mass and intermediate-mass stars will evolve to planetary nebulae, is more complicated. The most basic process which changes the surface chemical composition in AGB stars is the third dredge-up which follows thermal pulse (Iben & Renzini 1983). By this process ^{12}C and s-process elements are supplied to the surface of the star, and carbon stars and S-type stars may form (e.g. Smith & Lambert 1990). In addition the nucleosynthesis at the bottom of the convective envelope (hot bottom burning, hereafter HBB) may also influence the surface chemical composition in relatively high mass AGB stars. The most direct evidence of HBB is the existence of Li-rich S-type stars in the Magellanic clouds (Smith et al. 1995), which is supported theoretically by Sackmann & Boothroyd (1992).

The carbon, nitrogen and oxygen abundances and their isotopic ratios in red giants had been measured by Smith & Lambert (1985, 1986, 1990). Also the determination of these abundances has been tried for red giants in some globular clusters (e.g. Bri-

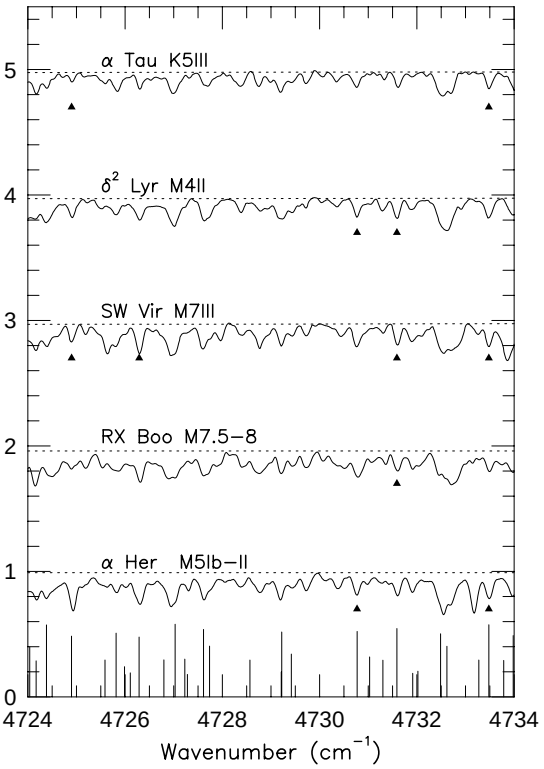

Fig. 1. Examples of normalized spectra in the K-window region. The filled triangles indicate CN lines used in our analyses. The solid lines at the bottom of the figure indicate lines of CN red system which dominate in this region.

ley et al. 1997). Now the abundance analysis should be done systematically from K to late M giants for the purpose of understanding the late stage of stellar evolution as well as the contribution to the chemical evolution of the Galaxy. The carbon abundance in M giants have been derived by the analyses of high resolution infrared spectra of CO lines by Tsuji (1991) and it was shown that the mean carbon abundance in late M giants are smaller by 0.3 dex than that in early M giants. This result suggests that further processing such as the CNO cycle should occur in late M giants and analyses of carbon, nitrogen and oxygen abundances in normal M giants would be required as well as those in S-type and carbon stars.

The high resolution spectra of CN and NH lines for M giants for which the carbon abundances have been derived by Tsuji (1991) are analyzed. The properties of these lines and the nitrogen abundance derived from those molecular lines are discussed in this paper.

2. Observations and mesurements

Observations of high resolution infrared spectra have been done by the Fourier transform spectrometer (FTS) of 4m telescope at Kitt Peak National Observatory (Hall et al. 1979). Spectra of oxygen-rich giants (including 5 M giants and 1 S-type star) in the *H*-window region and of 2 M giants in the *K*-window region were obtained on April 1982. Spectra in the *H*- and the *K*-window regions for 17 M and 2 K giants are also available from the archives. Further, spectra of 5 M giants in the *L*-window region were obtained on July and October 1987. The S/N ratio given in Table 1 is based on the peak signal level of the sum spectrum of two scans (forward and backward) and the root mean square of the difference spectrum. Examples of the spectra in the *K*- and the *L*-window regions are shown in Figs. 1 and 2, respectively, and details of these observations are summarized in Table 1. Thus we analyzed 2 K giants, 20 M giants and 1 S-type star in this work.

Table 1. Observations

(a) The observed stars (the H- and the K- window regions)

Star	Sp. Type	FWHM (cm^{-1})	S/N	Date of obs.
α Boo	K2III	0.059	290	Apr.15, 1979
α Tau	K5III	0.084	76	Sep.28, 1976
δ Oph	M0.5III	0.084	75	Jun.24, 1977
α Vul[(1)]	M0.5IIIb	0.070	70	Apr. 8, 1982
ν Vir[(2)]	M1III	0.070	115	Apr. 9, 1982
ν Vir[(1)]		0.070	79	Apr. 8, 1982
α Cet	M1.5III	0.084	69	Sep.28, 1976
β Peg	M2.5II-III	0.084	103	May.12, 1976
λ Aqr	M2.5III	0.084	61	Jul. 6, 1976
δ Vir	M3III	0.084	54	Jun.18, 1976
δ Vir		0.084	86	Jun.24, 1977
σ Lib	M3III	0.084	89	Aug.18, 1976
τ^4 Eri	M3.5III	0.084	59	Sep,29, 1976
10 Dra	M3.5III	0.084	61	Jun.28, 1977
BS1105[(1)]	S5,3	0.070	73	Apr. 8, 1982
δ^2 Lyr	M4II	0.084	78	Apr.11, 1976
ρ Per[(2)]	M4IIvar	0.038	66	Apr. 8, 1982
ρ Per[(1)]		0.038	54	Apr. 7, 1982
RR UMi	M5III	0.084	61	Aug.18, 1976
R Lyr[(1)]	M5III	0.050	121	Apr. 8, 1982
α Her	M5Ib-II	0.084	106	Jun.24, 1977
α Her		0.084	82	Feb.19, 1977
RZ Ari	M6IIIvar	0.084	88	Aug.17, 1976
30g Her	M6III	0.084	102	Jun.30, 1977
SW Vir	M7III:	0.084	65	Jun.18, 1976
EP Aqr[(1)]	M7III:	0.070	60	Apr. 8, 1982
RX Boo	M7.5-8	0.084	62	Jan.14, 1976

[(1)] Spectral range includes only the H- window region.
[(2)] Spectral range includes only the K- window region.

(b) The observed stars (the L- window-region)

Star	Sp. Type	FWHM (cm^{-1})	S/N	Date of obs.
α Her	M5Ib-II	0.0279	46	Jul. 9, 1987
RZ Ari	M6IIIvar	0.0279	50	Oct. 2, 1987
30g Her	M6III	0.0279	30:	Jul. 9, 1987
SW Vir	M7III:	0.0279	69	Jul. 9, 1987
RX Boo	M7.5-8	0.0279	88	Jul. 9, 1987

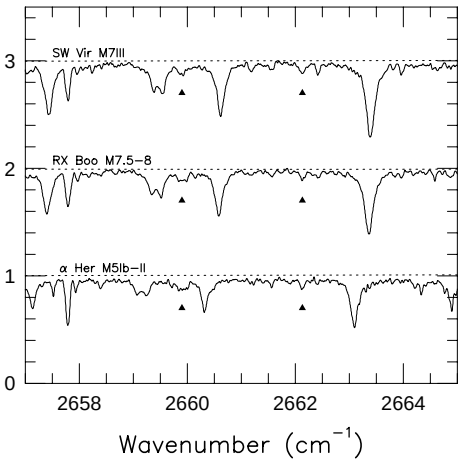

Fig. 2. Examples of normalized spectra in the L-window region. The filled triangles indicate NH lines used in our analyses.

Data reduction has been done by the same way as in Tsuji (1986a). We have used Norton & Beer's apodization function No.2 (Norton & Beer 1976) for which the full width at the half maximum (FWHM) of the instrumental line shape is given by FWHM = 0.8447/L (L is the maximum path difference of the interferometer) which is given in Table 1. We identified atmospheric absorption lines in the spectra by the use of the spectra of hot stars (Sun, Sirius, etc.), and used the lines that are little disturbed by atmospheric lines in our analyses.

For the purpose of determining nitrogen abundance we analyzed CN lines in the *H*- and/or the *K*-window regions for all stars. In addition, we analyzed NH lines in the *L*-window region for 5 stars which have spectral types later than M5, because the nitrogen abundance derived from CN lines depends directly on carbon abundance adopted in the analyses. All of our analyses were based on equivalent widths of these molecular lines. For determining the continuum level, the peak point of each 1024 data which are corresponding to 5-10 cm^{-1} is plotted against wavenumber and smooth curve is fitted to the higher points of these peaks. The equivalent widths of CN lines were measured by fitting Gaussian profile to each selected line. As the lines selected were fitted well by the Gaussian in the present work and line wings are generally not well defined in the spectra of cool stars, no improvement can be expected by the measurement with other methods (e.g. direct numerical integration of the line profile). In the case of NH lines, however, triplet structure of NH lines cannot be fully resolved into individual component though the spectral resolution is as high as $R = 10^5$. Therefore we measured equivalent widths for two or three components of the triplet structure together by the direct numerical integration of the profile. The equivalent widths measured are given in Table 10 [1].

Due to the high resolving power we can determine the intrinsic line width of CN. We measured the FWHMs of CN lines observed and plotted them against their depths after correcting for instrumental effect (Fig. 3). Note that the FWHM is transformed to the Gaussian dispersion in velocity unit (km/s). Then we determined the optically thin limit of the line width by extrapolating the plots to zero central depth. This optically thin limit can be interpreted as the intrinsic line width, which are summarized in Table 3 (5th column). These intrinsic line widths are used to constrain the micro-turbulent velocities (Sect. 4).

[1] Table 10 is only available in electronic form at the CDS via anonymous ftp to cdsarc.u-strasbg.fr (130.79.128.5) or via http://cdsweb.u-strasbg.fr/Abstract.html

Table 2. Physical parameters of model atmosphere

Star	$T_{\rm eff}$ (K)	Model used series/$T_{\rm eff}$/log$g$/$\xi_{\rm micro}$
α Boo	4375	–/4375/1.5/1.5[(1)]
α Tau	3860	G2/3900/1.5/3.0
δ Oph	3775	G2/3800/1.5/3.0
α Vul	3785	G2/3800/1.5/3.0
ν Vir	3795	G2/3800/1.5/3.0
α Cet	3905	G2/3900/1.5/3.0
β Peg	3580	G2/3600/1.0/3.0
λ Aqr	3835	G2/3800/1.5/3.0
δ Vir	3625	G2/3600/1.0/3.0
σ Lib	3575	G2/3600/1.0/3.0
τ^4 Eri	3695	G2/3700/1.0/3.0
10 Dra	3715	G2/3700/1.0/3.0
BS1105	3620	G2/3600/1.0/3.0
δ^2 Lyr	3385	G2/3400/0.5/3.0
ρ Per	3505	G2/3500/0.5/3.0
RR UMi	3355	G2/3400/0.5/3.0
R Lyr	3275	G2/3300/0.5/3.0
α Her	3220	G2/3200/0.0/3.0
RZ Ari	3295	G2/3300/0.5/3.0
30g Her	3235	G2/3200/0.0/3.0
SW Vir	3014	G2/3000/0.0/3.0
EP Aqr	3000:	G2/3000/0.0/3.0
RX Boo	3000:	G2/3000/0.0/3.0

(1) Frisk et al. (1982)

3. Input data

Generally there are four parameters, i.e. effective temperature ($T_{\rm eff}$), surface gravity (g), chemical composition and micro-turbulent velocity ($\xi_{\rm micro}$), in the analysis of equivalent widths of absorption lines. Chemical composition (i.e. nitrogen abundance in this work) and $\xi_{\rm micro}$ were determined from the analyses of absorption lines of CN and NH lines while $T_{\rm eff}$ and log g were estimated in advance by photometric data, stellar angular diameter and so on.

We adopted the same values of $T_{\rm eff}$ and log g of program stars as those in Tsuji (1986a, 1991). $T_{\rm eff}$ were determined by the use of the infrared flux method (IRFM, Blackwell et al. 1980) and/or from the stellar angular diameter (e.g. Ridgeway et al. 1982). The uncertainties of $T_{\rm eff}$ which should be considered

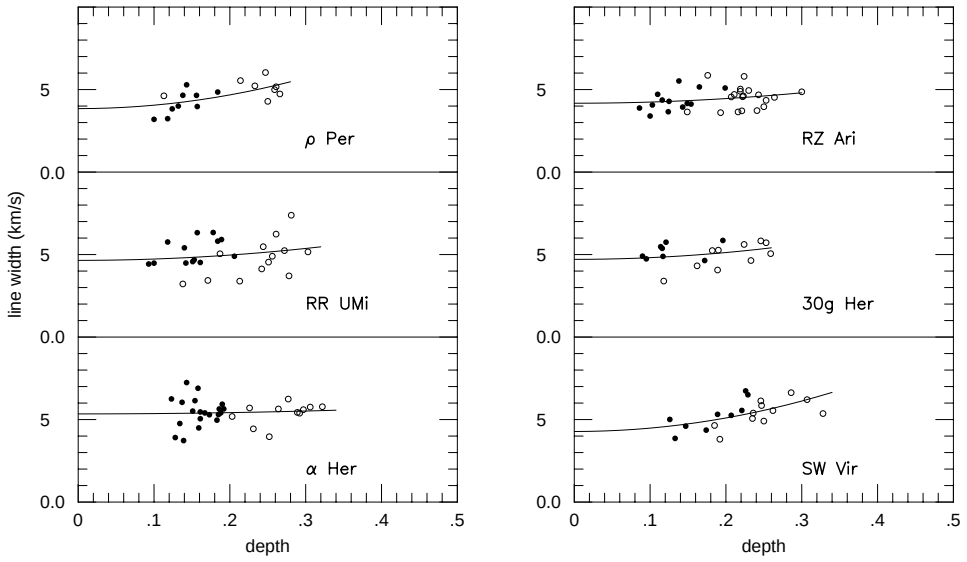

Fig. 3. Observed line widths (Gaussian dispersion (km/s)) after correcting for the effect of the instrumental broadening are plotted against the central depths. The lines of CN red system $\Delta v = -2$ and -1 sequences are represented by filled and open circles, respectively.

in the analysis are about 100K for most of the program stars and larger than 100K for some later type stars (RX Boo and EP Aqr). Surface gravities are derived by the assumption of $M = 3M_\odot$ which is a medium value of the possible mass range of evolved red giant stars ($1 \sim 10M_\odot$). Therefore the effect due to uncertainty of $\Delta\log g = \pm 0.5$ is examined later.

In the analysis we applied an extended version of the model atmospheres of series G2 (Tsuji 1978) which roughly represent a sequence of $3M_\odot$ stars. These models are calculated for the solar chemical composition and $\xi_{\rm micro} = 3$ km/s. For the K giant star α Boo, a model atmosphere of $T_{\rm eff} = 4375$ K by Frisk et al. (1982) was applied.

3.1. Molecular data

For the calculation of the line list of CN red system ($A^2\Pi - X^2\Sigma$, $\Delta v = -1$ and -2 sequences), we employed spectroscopic constants by Cerny et al. (1978) to calculate line positions, and Einstein's A coefficients by Bauschlicher et al. (1988). The determination of CN dissociation energy (D_0^0(CN)) has been a subject of controversy. Recently the values around 7.75 eV have been derived by many experiments, while smaller values (about 7.65 eV) have been derived by some theoretical works (see Lambert 1994, Costes & Naulin 1994). Sneden & Lambert (1982) derived smaller oscillator strengths of the CN red system than those by Bauschlicher et al. (1988) assuming D_0^0(CN)=7.65 eV, but the solar abundances of carbon and nitrogen adopted in their analyses were somewhat larger than the solar abundances determined by recent analysis (e.g. Grevesse et al. 1996). If these new abundances are adopted, the dissociation energy and/or the oscillator strength should be larger. In fact, a recent study of dissociation energy of CN from solar spectra by Sauval et al. (1994), who assumed larger oscillator strength than those by Bauschlicher et al. (1988), derived a larger dissociation energy (~ 7.85 eV). We adopted D_0^0(CN) = 7.75 eV as the CN dissociation energy in the present analysis.

For the line list of NH, we employed the line position by Boudjaadar et al. (1986) and the dipole moment of vibrational-rotational transition derived by Grevesse et al. (1990). We adopted $D_0^0 = 3.37$ eV as the dissociation energy of NH (Bauschlicher & Langhoff 1987).

4. Analysis of CN lines

4.1. Standard analysis

After a model atmosphere is specified by the effective temperature and surface gravity, chemical composition (i.e. nitrogen abundance in this work) and micro-turbulent velocity are determined by the analysis of spectral lines of CN molecule. If we assumed that micro-turbulent velocity is isotropic, Gaussian and depth-independent, the micro-turbulent velocity is determined so that nitrogen abundances from all the measured lines are consistent. We assumed the chemical composition except carbon and nitrogen to be solar and adopted the carbon abundance derived by Tsuji (1991) from weak lines of the CO second overtone bands.

Some examples of our analyses are shown in Fig. 4. We first assumed nitrogen abundance and micro-turbulent velocity, which specify equivalent width expected from the model atmosphere for each CN line. Next we searched for the corrections of line strengths of CN, Y's (see next paragraph), by which observed, equivalent width can be accounted for, and plotted them against $X = \log(W/\omega)_{\rm obs} + 6.0$. In Fig. 4 the open and filled circles indicate the results based on the lines analyzed in the H- and the K- window regions, respectively, and the solid lines indicate the function $Y = a + bX^2$ fitted to the circles. Then we can interpret the coefficient a to be the correction of line strength when we determine the micro-turbulent velocity so that the coefficient b becomes equal to zero.

The correction of line strength would be identical with the abundance correction of nitrogen, if the line strength of CN were proportional to the nitrogen abundance. However, in cool

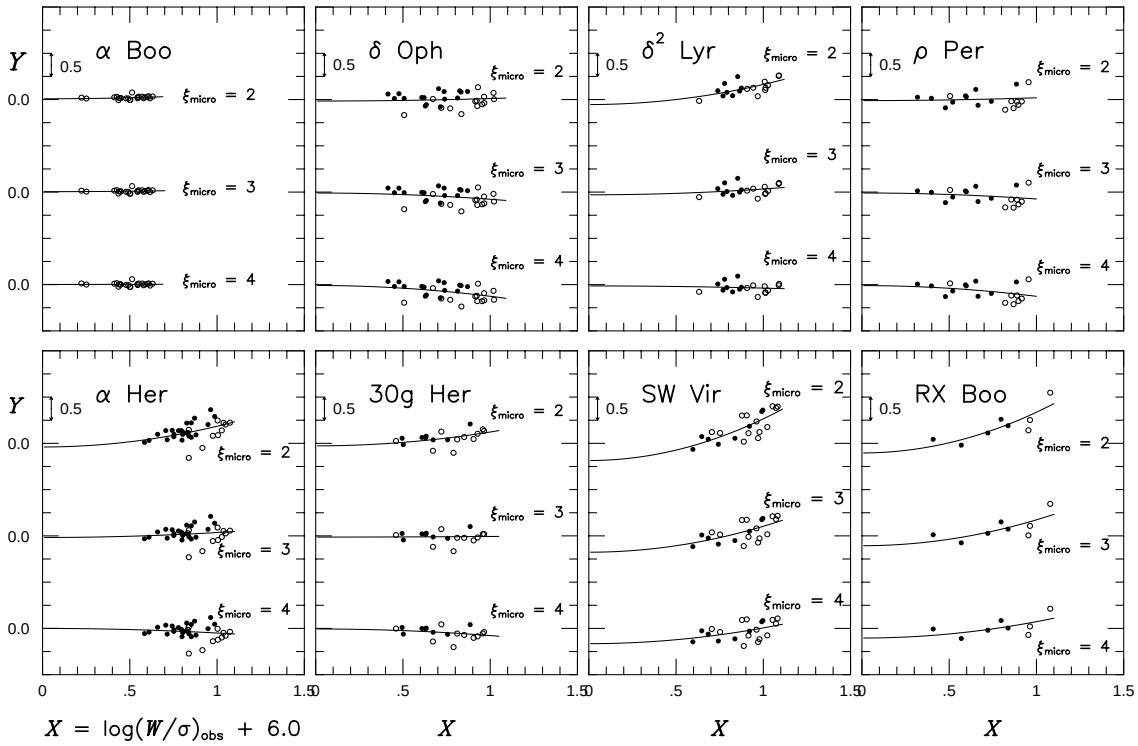

Fig. 4. Examples of standard analysis on CN lines. Corrections of line strengths of CN, Y's, are plotted against $X = \log(W/\omega) + 6.0$ where W is the observed equivalent width (in cm^{-1}) and ω is the wavenumber of the line (cm^{-1}). The lines of CN red system $\Delta v = -2$ and -1 sequences are represented by filled and open circles, respectively. Results are shown for three assumed values of micro-turbulent velocities; $\xi_{\mathrm{micro}} = 2$, 3 and 4 km/s at the top, middle, and bottom, respectively.

stars as M giants a great part of nitrogen atoms is bounded in N_2 molecules and then the correction of line strength of CN is not identical with the abundance correction of nitrogen. Indeed we found in the analysis that the relation between the correction of a line strength (Y) and the abundance correction of nitrogen in logarithmic scale ($\Delta\log A_{\mathrm{N}}$) is $Y \sim 0.8\,\Delta\log A_{\mathrm{N}}$ in our program stars. Therefore we iterated this analysis until the correction of line strength to be small enough. In Fig. 4 we show the examples in which the correction of line strength becomes small after two or three iterations. Results are summarized in Table 3 (6th and 7th columns for nitrogen abundance and micro-turbulent velocity, respectively), where the abundances ($\log A_{\mathrm{N}}$'s) are given on the scale of $\log A_{\mathrm{H}} = 12.0$.

As shown in Fig. 4 most of the lines analyzed are so weak that the dependence of equivalent widths on micro-turbulent velocities is small. This is a great advantage in determining abundance. On the other hand micro-turbulent velocities are not determined accurately. In fact we cannot derive reasonable values of micro-turbulent velocity for 8 stars. The derived micro-turbulent velocity of ν Vir is smaller than 1 km/s. For this star we assumed $\xi_{\mathrm{micro}} = 2$ km/s which is the typical value of red giants. The variations of the nitrogen abundance by the uncertainty of micro-turbulent velocity of ± 1 km/s are about 0.07 dex. On the other hand the micro-turbulent velocities of other 7 stars determined by the above method are very large (e.g. larger than 6 km/s). However the micro-turbulent velocity must be of course smaller than the velocity which is derived from the intrinsic line width in Sect. 2. Therefore we assumed the micro-turbulent velocities for these stars to be the velocities of the intrinsic line widths and determined the nitrogen abundances as the average of the abundance derived from all the lines. In order to estimate the uncertainty by this assumption, we also derive nitrogen abundances when we adopted the micro-turbulent velocities to be the same as that of CO absorption lines (the first overtone) determined by Tsuji (1986a) and compared them with the above results. The differences in the abundances are smaller than about 0.1 dex except for RX Boo and EP Aqr which show somewhat larger discrepancies of 0.25 dex and 0.4 dex, respectively.

4.2. Confirmation by empirical analysis

Since most of CN lines are weak and then not affected by saturation, it is possible to estimate nitrogen abundance by the use of the linear part of the curve-of-growth. We plotted observed equivalent widths against the predicted line strength ($\log\Gamma + \log gf$) calculated by the weighting function method (Cayrel & Jugaku 1963, and also the Appendix in Tsuji 1991). For weak lines the calculated line strength is equal to observed equivalent width when chemical composition of the star is assumed correctly. Some examples are shown in Fig. 5. The open and filled circles indicate the results based on the lines observed in the H-window region and those in the K-window region, respectively, as in Fig. 4. We find that most of the lines in the

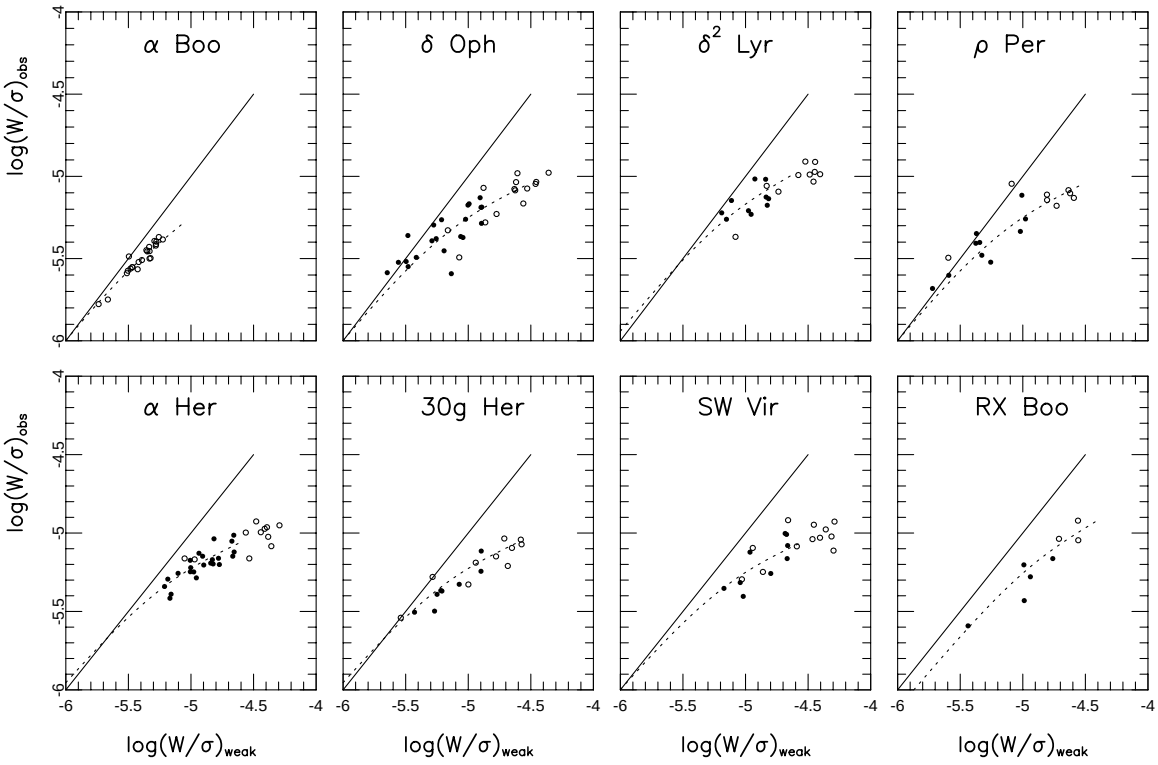

Fig. 5. Observed values of $\log(W/\omega)$ for CN lines are plotted against the theoretical line strengths (see Sect. 4.2). The lines of CN red system $\Delta v = -2$ and -1 sequences are represented by filled and open circles, respectively. Solid lines are the relations expected at the weak line limit for the nitrogen abundances obtained by the standard analysis outlined in Sect. 4.1.

H-window region are somewhat saturated in all stars except for α Boo while some of lines in the K-window region are in the linear part. Therefore it is somewhat difficult to determine the nitrogen abundance accurately by this method for the stars which were observed only in the H-window region (α Vul, BS1105, R Lyr and EP Aqr). The nitrogen abundances derived by this method are also shown in Table 3 (8th column). Generally speaking the agreement between the results by this method and those by the standard analysis is good except for EP Aqr which was observed only in the H-window region.

4.3. Uncertainties

We have already estimated the uncertainty of nitrogen abundance by the uncertainty of the micro-turbulent velocity in Sect. 4.1. In this section we estimate the uncertainties by other factors.

The internal errors, which were estimated from the probable errors of the nitrogen abundances determined for all lines, are shown in Table 3 with the results of nitrogen abundances (6th column). These errors are larger in the stars for which we could not determine the micro-turbulent velocity and used assumed values (see Sect. 4.1). Two different spectra are available for the same object (δ Vir and α Her) and we compared the equivalent widths of common lines as well as the nitrogen abundance derived independently from each spectrum (Table 4). The agreement of nitrogen abundance derived from the two spectra of δ Vir is good. On the other hand the discrepancy of nitrogen abundance derived from the two spectra of α Her is somewhat large (0.20 dex). However this discrepancy can be explained by the fact that we can use only 7 lines for one of the spectra of this star.

In the analysis of CO lines in Tsuji (1986a, 1991) it was shown that there is a difference between the carbon abundance as well as the micro-turbulent velocity derived by the first overtone of CO in the K-window region and those by the second overtone in the H-window region. Therefore we compared the nitrogen abundance derived by the analysis in the K-window region (lines of $\Delta v = -2$) with those by the analysis in both the H- and the K-window regions (including both $\Delta v = -1$ and -2 lines) for 19 stars which have been observed in both window regions. The differences of nitrogen abundance are about 0.1 dex or smaller and we conclude that the results by both analyses agree well. The reason of the discrepancy between the carbon abundances derived from the first and second overtone of CO noted in Tsuji (1991) has not been clear yet, but our results of the nitrogen abundance will be free from this kind of ambiguity.

One of the large difficulties in determination of the nitrogen abundance from CN lines is that the results are directly influenced by the uncertainty of the carbon abundance adopted in the analysis. The uncertainty of the carbon abundance derived by Tsuji (1991) is about 0.2 dex which is mainly related to the uncertainty of model parameters, especially of surface gravity. We estimated the influences by changing the carbon abundance

Table 3. Results by lines of CN red system

Star	log A_C	ξ_{CO} (km/s)	N_{line}	ξ_{obs} (km/s)	log A_N	ξ_{CN} (km/s)	log A_N by COG
α Boo	8.06	2.22	23	4.2±0.1	7.77±0.02	4.2±2.0	7.8
α Tau	8.39	2.20	38	3.9±0.1	8.05±0.03	2.5±0.4	8.1
δ Oph	8.38	3.18	30	4.1±0.2	8.40±0.06	2.2±0.3	8.4
α Vul	8.35	9.7[(1)]	12	4.7±0.5	7.90±0.10	5.0[(3)]	8.0
ν Vir	8.23	2.80	12	4.3±0.5[(2)]	7.97±0.12	2.0[(4)]	8.0
α Cet	8.57	3.60	35	4.8±0.2	7.84±0.05	3.1±0.4	7.9
β Peg	8.24	3.12	36	4.9±0.5	8.16±0.04	1.4±0.3	8.1
λ Aqr	8.37	3.56	26	4.7±0.3	8.23±0.07	1.3±0.4	8.2
δ Vir	8.49	2.66	32	4.4±0.7[(2)]	7.96±0.07	2.4±0.4	8.0
	8.49	2.66	24	4.3±0.2	7.85±0.12	4.0[(3)]	7.9
σ Lib	8.23	3.04	23	5.0±0.3	8.15±0.05	2.1±0.3	8.2
τ^4 Eri	8.35	2.70	19	4.5±0.2	8.04±0.05	2.9±0.6	8.2
10 Dra	8.20	3.36	30	4.3±0.2	8.47±0.07	4.0±0.9	8.6
BS 1105	8.46	2.9[(1)]	20	4.4±0.3[(2)]	8.34±0.11	2.7±0.3	8.4
δ^2 Lyr	8.05	4.06	18	5.5±0.2	8.65±0.08	4.0±0.5	8.7
ρ Per	8.10	2.68	18	3.9±0.2	8.40±0.07	2.2±0.4	8.4
RR UMi	8.17	2.72	26	4.6±0.3	8.20±0.06	5.5±1.0	8.3
R Lyr	8.18	3.7[(1)]	11	4.9±0.6	8.18±0.12	5.0[(3)]	8.2
α Her	8.05	3.30	34	5.4±0.2	8.66±0.08	3.5±0.4	8.7
	8.05	3.30	7	5.7±0.9	8.46±0.12	6.0[(3)]	8.6
RZ Ari	7.97	2.72	33	4.2±0.2	8.62±0.07	3.0±0.6	8.6
30g Her	7.99	3.20	18	4.7±0.2	8.43±0.06	3.1±0.5	8.5
SW Vir	8.26	3.60	21	4.4±0.3	8.46±0.16	4.0[(3)]	8.5
EP Aqr	8.07	3.3[(1)]	7	5.7±0.3[(2)]	8.48±0.10	6.0[(3)]	8.7
RX Boo	8.00	2.68	8	5.1±0.7[(2)]	8.77±0.14	5.0[(3)]	8.7

(1) Derived from weak lines of CO second overtone (Tsuji 1991).
(2) Average of CN line widths.
(3) These ξ_{micro} are estimated from ξ_{obs} (see Sect. 4.1).
(4) Assumed value. The micro-turbulent velocity determined by standerd analysis is lower than 1 km/s (Sect. 4.1).

Table 4. Comparison of the results and equivalent widths for t wo spectra

δ Vir	adopted	the other	Δ log A_N
	log A_N=7.96	log A_N=7.85	0.11
Line	log(W/λ)		Δlog(W/λ)
2-4 Q_1 19	−5.244	−5.355	+0.111
1-3 P_2 24	−5.359	−5.419	+0.060
0-2 Q_1 46	−5.221	−5.204	−0.017
1-2 R_2 68	−5.279	−5.207	−0.072
0-1 Q_2 64	−5.174	−5.111	−0.063
α Her	adopted	the other	Δ log A_N
	log A_N=8.66	log A_N=8.46	0.20
Line	log(W/λ)		Δlog(W/λ)
1-3 Q_1 44	−5.037	−5.175	−0.138
1-3 Q_2 44	−5.197	−5.232	+0.035
1-3 Q_2 29	−5.121	−5.223	+0.102

Table 5. Effects of uncertainties in carbon abundances

Δ log A_C	τ^4 Eri	30g Her
	log A_C=8.35 log A_N=8.04	log A_C=7.99 log A_N=8.43
−0.20	+0.30	+0.26
+0.20	−0.35	−0.25

assumed and show them in Table 5. The uncertainty of the nitrogen abundance (about 0.25 dex or somewhat larger) is larger than that of carbon abundance assumed (0.2 dex). One of the reasons is that a great part of nitrogen atoms is bounded in N_2 molecules while most of carbon atoms are bounded in CO molecules in cool stars as M-giants, and the variation of CN line strength is not so sensitive to the change of the nitrogen abundance as to that of the carbon abundance.

The uncertainties of the nitrogen abundances by uncertainties of physical parameters assumed are also estimated by varying effective temperature or surface gravity. The uncertainty of

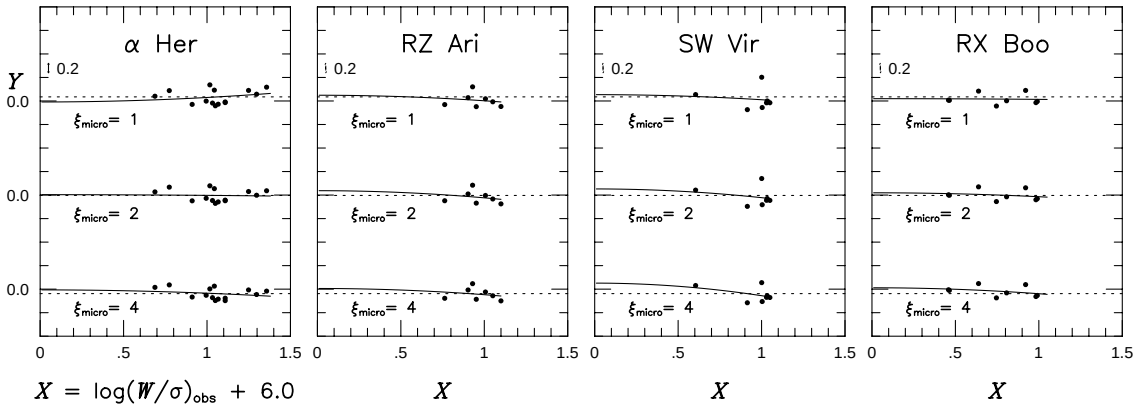

Fig. 6. Examples of standard analysis on NH lines. Corrections of line strengths of NH, Y's, are plotted against $X = \log(W/\omega) + 6.0$. The lines of NH are represented by circles. The dotted lines indicate the average of Y's. Results are shown for three assumed values of micro-turbulent velocities; $\xi_{\rm micro} = 1$, 2 and 4 km/s at the top, middle, and bottom, respectively.

effective temperature is about 100K or larger and that of surface gravity is about a factor of 3 as noted in Sect. 3.1. To estimate the effects of these uncertainties, we have done the standard analyses again for τ^4 Eri and 30g Her by varying effective temperature by $\Delta T_{\rm eff} = 100$K or surface gravity by $\Delta \log g = 0.5$ dex. The results are summarized in Table 6 (3rd and 5th column for τ^4 Eri and 30g Her, respectively). By this estimation the effect of the uncertainty of surface gravity is larger than that of effective temperature. However we must consider again the influence of the variation of the carbon abundance which is caused by the variation of physical parameters. The variation of the carbon abundances due to the variations of parameters are summarized in Tsuji (1991) as follows; $\Delta A_{\rm C} = \pm 0.06$ dex for $\Delta T_{\rm eff} = \pm 100$ K and $\Delta A_{\rm C} = \pm 0.20$ dex for $\Delta \log g = \pm 0.5$ dex. We investigated again the effects of variation of parameters considering these variation of the carbon abundance and obtained the results as shown in Table 6 (4th and 6th column for τ^4 Eri and 30g Her, respectively). We find that the uncertainties of the nitrogen abundance by surface gravity is canceled out to some extent, while the uncertainty by effective temperature is enlarged.

The other large difficulty in the analysis of CN lines is the uncertainty of the dissociation energy of CN molecule which may produce systematic error in the nitrogen abundance. The effects of this uncertainty on the nitrogen abundance is estimated to be $\Delta \log A_{\rm N} \sim -0.15$ for $\Delta D_0^0({\rm CN}) = +0.10$ eV. The difference of this effect by stellar temperature is not large.

5. Analysis of NH lines

5.1. Standard analysis and uncertainties

The analysis of NH lines was done in the same way as that of CN lines. In this case the calculated equivalent widths were obtained by the direct integration of synthetic spectrum for two or three components of the triplet structure as the measurement of observed equivalent widths (see Sect. 2).

Examples of the analyses are shown in Fig. 6. The definitions of axes and solid lines in this figure are the same as in Fig. 4. The dashed lines indicate the average of corrections of line strengths. Because most of the values of equivalent widths shown in Fig. 6 are those of three components, the equivalent width corresponding to single component is about one third of that in Fig. 6. Therefore the saturation effect will be very small in this case and the uncertainty of the nitrogen abundance caused by micro-turbulent velocity is negligible compared with the internal error.

The correction of line strength of NH in this analysis is proportional to the square root of the correction of the nitrogen abundance, i.e. $Y \sim \frac{1}{2}\Delta \log A_{\rm N}$. This fact means that most of nitrogen atoms are bounded in N_2 molecules in the layers of atmosphere where NH lines form. We iterated this analysis until the abundance correction becomes sufficiently small as the analysis of CN lines.

The results of this analysis and internal errors are shown in Table 7. The internal errors are between 0.15 and 0.25 dex, which are larger than those in the analysis of CN lines. The reasons of these large internal errors are not only the difficulty in the measurement of equivalent widths of NH lines but also the sensitivity of the nitrogen abundance to the NH line strength.

In the analysis of NH lines the effect of uncertainty of the carbon abundance adopted is negligible. The effects of uncertainties of physical parameters (effective temperature and surface gravity) for α Her are estimated as shown in Table 8. These uncertainties are smaller than the internal error in this case.

5.2. Comparison with the results based on CN

By the above analyses we can derive the nitrogen abundances from both CN and NH lines independently for 5 stars. These results are compared in Fig. 7. We find that the nitrogen abundances by the analyses of NH lines agree well with those by CN lines except for RX Boo, for which the nitrogen abundance derived from CN lines is larger by 0.37 dex than that from NH line. However there is a difficulty in the analysis of this star related to the uncertainty of micro-turbulent velocity as noted in Sect. 4.1. The physical parameters of this star are more uncertain than those of other stars as noted in Sect. 3, though recent

Table 6. Effects of uncertainties in physical parameters

Assumed uncertainties		Resulting uncertainties $\Delta \log A_N$			
ΔT_{eff}	$\Delta \log g$	τ^4 Eri		30g Her	
		$\Delta \log A_C$ considered		$\Delta \log A_C$ considered	
+100	0.0	−0.02	−0.11	−0.02	−0.08
0.0	+0.5	+0.19	−0.15	+0.19	−0.07

Table 7. Results by NH lines

Star	ξ_{CO} (km/s)	log A_N by ξ=2.0	log A_N by ξ=4.0	N_{line}	log A_N adopted	log A_N by CN
α Her	3.30	8.78±0.17	8.61	14	8.8	8.66
RZ Ari	2.72	8.40±0.19	8.30	7	8.4	8.62
30g Her	3.20	8.25±0.15	8.05	9	8.3:	8.43
SW Vir	3.60	8.42±0.27	8.27	7	8.4	8.46
RX Boo	2.68	8.40±0.15	8.31	8	8.4	8.77

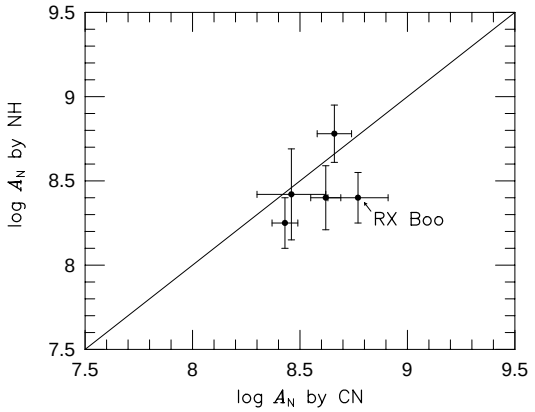

Fig. 7. The comparison between the nitrogen abundances derived from CN and NH lines for 5 stars.

determination of T_{eff} from angular diameter (2943K by Dyck et al. 1996) supported the T_{eff} adopted in this work (3000K). Further RX Boo is known to be semiregular variable and this fact may produce some other uncertainty in abundance analysis. Excluding RX Boo by the reasons mentioned above, we find that the mean of the nitrogen abundances determined by CN lines is larger by about 0.08 dex than that by NH lines for other 4 stars. This discrepancy is within the errors estimated in the above sections and then we conclude that the agreement between the analyses of CN and of NH is fine.

We should note, however, that the dissociation energy of CN molecule affect this comparison. If we adopt the lower value of the dissociation energy of CN, the discrepancy between the nitrogen abundacnes from CN and NH becomes larger; e.g. the discrepancy is 0.23 dex if D_0^0=7.65 eV is adopted.

Table 8. Effects of uncertainty in physical parameters

Assumed uncertainties		Resulting uncertainties
ΔT_{eff}	$\Delta \log g$	$\Delta \log A_N$ (α Her)
+100	0.0	+0.04
0.0	+0.5	+0.14

Table 9. Comparison with other authors

Name	Present			Smith & Lambert 1990a	
	log A_N	log $A_N^{(1)}$	log A_C	log $A_N^{(2)}$	log A_C
α Tau	8.05	8.18	8.39	8.20	8.40
α Vul	7.90	8.06	8.35	8.23	8.51
ν Vir	7.97	8.11	8.23	8.22	8.51
β Peg	8.16	8.29	8.24	8.18	8.42
δ Vir	7.96	8.09	8.49	8.21	8.61
10 Dra	8.47	8.61	8.20	8.28[(3)]	8.59
ρ Per	8.40	8.53	8.10	8.26[(4)]	8.46
30g Her	8.43	8.56	7.99	8.45	8.25

(1) ^{14}N abundances derived when D_0^0(CN) = 7.65 eV is adopted.
(2) ^{14}N abundances from CN except for the stars with other superscripts.
(3) ^{14}N abundances from NH only.
(4) ^{14}N abundances are an average from CN and NH.

6. Discussion

6.1. Comparison with other authors

In Table 9 we compare our results on the nitrogen abundance as well as the carbon abundance with those in Smith & Lambert (1990) who analysed 8 stars in common with us. In Smith & Lambert (1990) the nitrogen abundances were derived from lines of CN red system and/or NH vibrational-rotational lines. The dissociation energy of CN adopted by them was D_0^0(CN) = 7.65 eV, which is smaller by 0.1 dex than

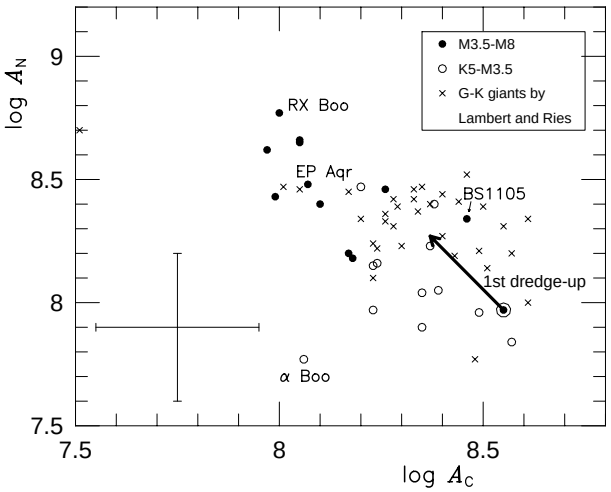

Fig. 8. The nitrogen abundances determined by the analysis of CN lines are plotted against the carbon abundances determined by Tsuji (1991). The open and filled circles indicate early M giants (including two K giants, α Boo and α Tau) and late M giants, respectively, which are analyzed in the present work. The uncertainties in the worst case of nitrogen and carbon abundances estimated in Sect. 4 and in Tsuji (1991), respectively, are shown by error bars. Crosses mean the abundances of G and K giants determined by Lambert & Reis (1981). Solar abundance is also plotted. The arrow indicates the variation in the carbon and nitrogen abundances through the first dredge-up expected for a star with the solar abundance.

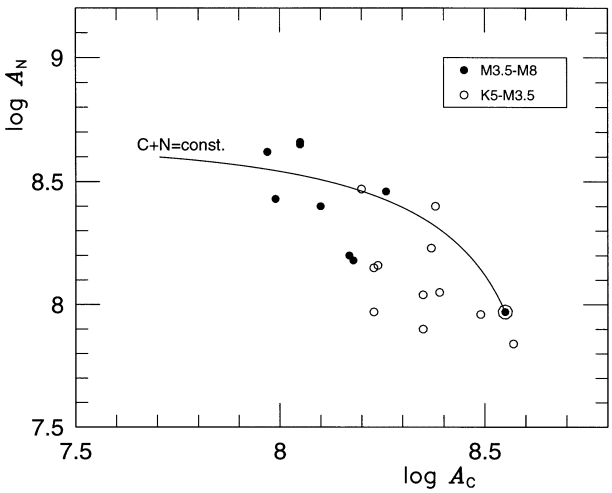

Fig. 9. The nitrogen and carbon abundances are shown as Fig. 8. The solid line indicates the variation in the carbon and nitrogen abundances by the CN cycle starting from the solar abundances.

that in our analyses. Therefore we also show in Table 9 the nitrogen abundance derived from CN lines when we assume D_0^0(CN) = 7.65 eV, and compare them with the results of Smith & Lambert (1990).

Our result of the nitrogen abundance of K giant α Tau agrees very well with that of Smith & Lambert (1990) as well as the carbon abundance. For this star we analyzed the equivalent widths of CN lines listed in Smith & Lambert (1985, the results of the paper have been compiled in their 1990 paper) by the same method of the present analysis and obtained the consistent result with that of Smith & Lambert. On the other hand, for 30g Her, the nitrogen abundance by the present analysis is higher than that in Smith & Lambert (1990) by 0.11 dex while the carbon abundance adopted in the present analysis is lower by 0.26 dex than that in Smith & Lambert (1990). For this star we also analyzed the equivalent widths of CN lines listed in Smith & Lambert (1985) and obtained $A_N = 8.50$, which is consistent with our result. Therefore we conclude that the difference of the resulted nitrogen abundances is not caused by the measurement or selection of CN lines.

It is not simple to compare the carbon and nitrogen abundances simultaneously, but we find that the present results of carbon and nitrogen abundances are consistent with Smith & Lambert (1990) for 5 earlier type stars, while the carbon abundances are lower and the nitrogen abundances are higher in the present results than those in Smith & Lambert (1990) for other 3 later type stars.

6.2. Carbon and nitrogen abundance in M giants

By the present analyses and Tsuji (1991) we can discuss the carbon and nitrogen abundance in 23 oxygen-rich cool giants. The results are plotted in Fig. 8 where horizontal and vertical axes indicate the carbon and nitrogen abundances, respectively. The open and filled circles indicate the stars earlier than M3.5 and later than M4, respectively. The solar abundances (log $A_C = 8.55$ and log $A_N = 7.97$ by Grevesse et al. 1996) are shown by the symbol $\odot$. It should be noted that the uncertainties of the nitrogen abundance of RX Boo and EP Aqr are larger than those of other stars (Sect. 4). We find that both carbon and nitrogen abundances are small in the K giant, α Boo, which is known to be metal poor. On the other hand S-type star BS1105 is located in the region with high abundances of both carbon and nitrogen. This is consistent with the trend of abundances in typical S-type stars (Smith & Lambert 1990). We exclude these four stars from the following discussion.

The arrow in Fig. 8 indicates the change of carbon and nitrogen abundances expected by the first dredge-up in the star whose initial abundance is assumed to be the solar. This change was summarized in Iben & Renzini (1983) as follows; carbon abundance decreases by about 30 % and nitrogen abundance increases by about a factor of two for the star which has initially the solar abundances. We find that about a half of our program stars, most of which are earlier than M4, have the carbon and nitrogen abundances expected by the first dredge-up, but others (later than M4) show larger decrease of carbon as well as larger increase of nitrogen than those expected from the first dredge-up. Here the uncertainty of abundances which is shown in Fig. 8 by error bar for the worst case must be considered, but at least some of late M giants have lower carbon abundance as well as higher nitrogen abundance than those expected by the first dredge-up (shown by the tip of the arrow in Fig. 8). This can be shown clearly by the comparison with the abundance in G and K giants shown in Fig. 8 by crosses. These abundances

have been derived by Lambert and Ries (1981) from C_2, CN and [OI] lines and interpreted to be the observational evidence for the first dredge-up. In fact most of G-K giants distribute around the point expected from the first dredge-up as are the early M giants. We conclude that carbon and nitrogen abundance in early M giants can be well explained by the theory of the first dredge-up but these abundances in late M giants show a variation from those in early M giants.

This conclusion is mainly due to the marked reduction of the carbon abundances in late M giants by Tsuji (1991) because the nitrogen abundances determined by CN lines are dependent on the carbon abundance adopted in the analysis. However it is unlikely that the carbon abundance determined from the weak lines of second overtone of CO is in large systematic errors, since almost all the carbon is locked in CO in late M giants and the carbon abundance is almost free from the errors in transformation from CO abundance to carbon abundance. It is also interesting that the oxygen isotope ratio ($^{16}O/^{17}O$) shows systematically low values in late M giants ($100 \sim 250$) compared with early M giants (~ 1000) (Tsuji 1986b).

Then we investigate what kind of nucleosynthetic process is responsible to the abundances of carbon and nitrogen in late M giants. In Fig. 9 the solid line indicates the change of carbon to nitrogen due to the CN cycle starting from the solar abundances. The carbon and nitrogen abundances of late M giants can be explained well by this abundance change. This means that the effect of He burning and subsequent HBB which are expected in AGB stars does not emerge clearly even in late M giants and the abundance feature of carbon and nitrogen may be explained by hydrogen burning (the CNO cycle) alone. This is also consistent with the result of the oxygen isotope ratio ($^{16}O/^{17}O$) which is considered to decrease by the CNO cycle (Tsuji 1986b).

From the above discussion of the carbon and nitrogen abundances we presume that additional conversion from carbon to nitrogen by the CN cycle and mixing of the products to the surface are required during the evolution after the first dredge-up, probably on the AGB, considering their late spectral type and high luminosity (Table 5 in Tsuji 1991). Many observations and theoretical calculations of stellar evolution have been done concerning the CN cycle and mixing after the first dredge-up. For example; some low-mass red giants show lower $^{12}C/^{13}C$ ratio (< 10) than that expected from the first dredge-up ($20 \sim 30$) (e.g. Gilroy 1989); There is a group of G and K giants called "weak G-band star" (Sneden et al. 1978) which has low carbon and high nitrogen abundances and very low $^{12}C/^{13}C$ ratio (~ 3, i.e. equilibrium value of the CN cycle). The problem of $^{12}C/^{13}C$ ratio in G-K giants may be explained by the meridional circulation during the evolution on red giant branch after the first dredge-up (Charbonnel 1995). However the carbon and nitrogen abundances in late M giants may not be explained by this hypothesis because these M giants may not remain so long on red giant branch as to be affected by such a slow process as the meridional circulation. There is also a calculation of mixing in AGB stars which brings about a change of the carbon and nitrogen abundances (Wasserburg et al. 1995). This calculation predicts very low $^{12}C/^{13}C$ ratio and large nitrogen enrichment by a factor of $3 \sim 6$ and may be appropriate to explain our results.

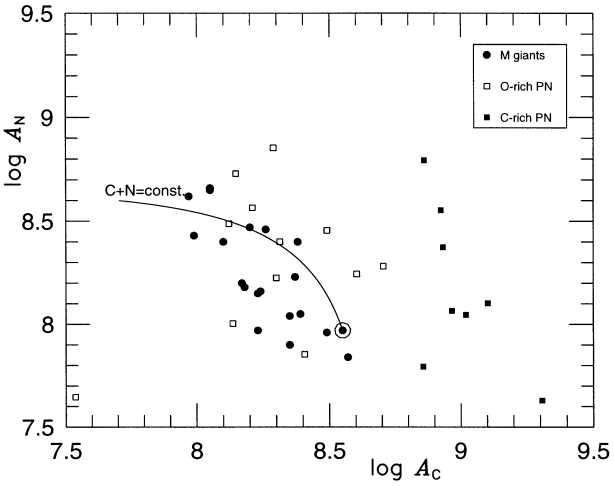

Fig. 10. The nitrogen and carbon abundances are plotted as Fig. 9. All M giants are shown by filled circles in this figure. Open and filled squares indicate the abundances of oxygen-rich and carbon-rich planetary nebulae, respectively, determined by Kingsburgh & Barlow (1994).

Low-mass and intermediate-mass stars as our program stars are considered to evolve to planetary nebulae (PNe) through mass-loss, but the details of evolution from stars to PNe have not been clarified yet. Our results of M giants are compared with the carbon and nitrogen abundances of PNe derived by Kingsburgh & Barlow (1994) in Fig. 10, where oxygen-rich and carbon-rich PNe are shown by the open and filled squares, respectively. Other symbols have the same meaning as in Fig. 8. Kingsburgh & Barlow (1994) combined UV spectra with optical spectra and thus covered a wide range of ionization stages for each element. We find that the distribution of oxygen rich PNe extends to carbon poor, nitrogen rich region in Fig. 10 and is consistent with the distribution of M giants. The origin of both carbon-rich and oxygen-rich PNe is discussed in Smith & Lambert (1990), but remains as a kind of puzzle. Our results cover only oxygen-rich stars, but we can at least conclude that the distribution of M giants including very low carbon and high nitrogen abundances is consistent with the hypothesis that M giants evolve to oxygen-rich PNe. To understand the evolution from stars to PNe completely, the comprehensive and systematic studies of various kinds of cool stars are necessary.

7. Concluding remarks

The analyses of high resolution infrared spectra have been done for CN lines in oxygen-rich cool evolved stars including 2 K giants, 20 M giants and 1 S-type star. For 5 later M giants NH lines have also been analyzed. We determined the nitrogen abundances from CN and/or NH weak lines which are appropriate to abundance analysis. The nitrogen abundances derived from NH lines for late M giants agree well with those from CN lines within the errors of our analyses, when we adopt 7.75 eV as the dissociation energy of CN molecule. The results show that the

nitrogen abundances in late M giants are larger than those in early M giants as opposed to the feature of carbon abundance (Tsuji 1991). These variation of abundances can be explained if we assume additional CN cycle and mixing after the first dredge-up, probably on AGB. However, such variation of carbon and nitrogen abundances cannot be predicted by the present evolutionary model of low-mass and intermediate-mass stars.

The evolution of light elements such as carbon and nitrogen in the Galaxy still remains an open question. Especially the origin of nitrogen is probably complex because nitrogen is the secondary element, i.e. the production follows the preceding synthesis of carbon which is also not simple. Nitrogen are considered to be produced in massive stars which evolve to supernovae as well as in low-mass and intermediate-mass stars by the CNO cycle, but their contributions to the chemical evolution of the Galaxy are not resolved quantitatively. Our results which show high nitrogen abundance in late M giants would be one of the bases to understand the origin of nitrogen. On the other hand it is important to investigate nitrogen abundances in unevolved stars which trace the Galactic chemical evolution.

To clarify the relation between chemical composition derived by our works and the chemical evolution of the Galaxy, the most important process is the mass-loss of these evolved stars. For the study of mass-loss, infrared spectroscopy is indispensable, and some of our program stars in this work are included in our observation program by the infrared space observatory (ISO). For interpretation of ISO spectra, detailed analysis of high resolution spectra as this work gives basic informations such as stellar abundance and atmospheric parameters.

Acknowledgements. We are grateful to Drs. K.H. Hinkle and S.T. Ridgeway for their kind advice in carrying out observations with the FTS at Kitt Peak as well as for making available the spectra of cool stars from the archives of KPNO. We thank the referee, Dr. J.P. Maillard, for valuable comments and suggestions for improving this paper.

References

Baushlicher C.W.Jr., Langhoff S.R., 1987, Chem. Phys. Lett., 135, 67
Baushlicher C.W.Jr., Langhoff S.R., Taylor P.R., 1988, ApJ 332, 531
Blackwell D.E., Petford A.D., Shallis M.J., 1980, A&A 82, 249
Boudjaadar D., Brion J., Chollet P., Guelachvili G., Vervloet M., 1986, J. Mol. Spectrosc. 119, 352
Briley, M.M., Smith, V.V., King, J., Lambert, D.L., 1997, AJ 113, 306
Cayrel R., Jugaku J.,1963, Ann. d'Astrophys. 26, 495
Cerny D., Bacis R., Guelachvili G., Roux F., 1978, J. Mol. Spectrosc. 73, 154
Charbonnel C., 1995, ApJ 453, L41
Costes M., Naulin C., 1994, in 'Molecules in the Stellar Environment' ed. U.G. Jørgensen, Springer-Verlag, 250
Dyck H.M., Benson, J.A., van Belle G.T., Ridgway S.T., 1996, AJ 111, 1705
Frisk U., Bell R.A., Gustafsson B., Nordh H.L., Olofsson S.G., 1982, MNRAS 199, 471
Gilroy K.K., 1989, ApJ 347, 835
Grevesse N., Lambert D.L., Sauval A.J., Dishoeck E.F., Farmer C.B., Norton R.H., 1990, A&A 232, 225
Grevesse N, Noels A., Sauval A.J., 1996, in ASP Conf. Ser. 99 'Cosmic Abundances', eds. S.S. Holt, G. Sonneborn, 117
Hall D.N.B., Ridgway S.T., Bell E.A., Yarborough J.M., 1979, Proc. Soc. Photo-Opt. Instrum. Engineers 172, 121
Iben I.Jr., Renzini A., 1983, ARAA 21, 271
Kingsburgh R.L., Barlow M.J., 1994, MNRAS 271, 257
Lambert D.L., 1994, in 'Molecules in the Stellar Environment' ed. U.G. Jørgensen, Springer-Verlag, 1
Lambert D.L., Ries L.M., 1981, ApJ 248, 228
Norton R.M., Beer R., 1976, J. Opt. Soc. America, 66, 259
Ridgway, S.T., Jacoby, G.H., Joyce, R.R., Siegel, M.J., Wells, D.C., 1982, AJ 87, 808
Sackmann, I.-J., Boothroyd, A.I., 1992, ApJ, 392, L71
Sauval A. J., Blomme R., Grevesse N., 1994, in 'Poster session Proceedings of IAU Coll. 146', eds. P. Thejll & U.G. Jørgensen, 107
Smith V.V., Lambert D.L., 1985, ApJ 294, 326
Smith V.V., Lambert D.L., 1986, ApJ 311, 843
Smith V.V., Lambert D.L., 1990, ApJS 72, 387
Smith V.V., Plez B., Lambert D.L.,Lubowich D.A., 1995, ApJ 441, 735
Sneden C., Lambert D.L., 1982, ApJ 259, 381
Sneden C., Lambert D.L., Tomkin J., Peterson R.C., 1978, ApJ 222, 585
Tsuji T., 1978, A&A 62, 29
Tsuji T., 1986a, A&A 156, 8
Tsuji T., 1986b, Ap&SS 118, 227
Tsuji T., 1991, A&A 245, 203
Wasserburg G.J., Boothroyd A.I., Sackmann I.-J., 1995, ApJ 447, L37

This article was processed by the author using Springer-Verlag LaTeX A&A style file *L-AA* version 3.